Food Chemistry 313 (2020) 126154

Contents lists available at ScienceDirect

Food Chemistry

journal homepage: www.elsevier.com/locate/foodchem

Development of a scalable procedure by a discontinuous crossflow DF/UF to obtain a concentrate of chenopodin from a dead-end centrifugal UF at bench scale

Migdalia Arazo[a,*], Nestor Jaque[a], Nelson Caro[b], Lilian Abugoch[a,*], Cristian Tapia[a,*]

[a] Departamento de Ciencia de los Alimentos y Tecnología Química, Facultad de Ciencias Químicas y Farmacéuticas, Universidad de Chile, Santos Dumont 964, Santiago, Chile

[b] Centro de Investigación AustralBiotech, Universidad Santo Tomás, Av. Ejército Libertador 146, Torre C, Nivel-2, Santiago, Chile

ARTICLE INFO

Keywords:
Quinoa protein
Ultra15 centrifugal filter devices
Crossflow filtration
Diafiltration
Ultrafiltration
Membrane fouling mechanism
Scaling-up procedures

ABSTRACT

The aim of this study was to develop a scalable crossflow diafiltration/ultrafiltration procedure for quinoa 11S globulin purification starting at the bench scale using Ultra15 centrifugal filter devices. The electrophoretic profiles of centrifugal ultrafiltration fractions showed a high heterogeneity in the bands, while crossflow ultrafiltration reduced the phenomena of protein sticking to the membrane, avoiding aggregate formation. In the crossflow protein concentration, flux decline curves were studied according to Hermia's fouling mechanisms and the resistance in a series model. High reversible resistance was related to external mechanisms due to complete blockage of the membrane surface followed by cake formation. The crossflow ultrafiltration was the most efficient technique for obtaining 57 kDa chenopodin isolate with higher processing capacity, purity and protein yield. The diafiltration/ultrafiltration process proved to be adequate and easy to handle to scale up the production of the 11S quinoa globulin.

1. Introduction

Proteins from plant sources have a high applicability in various processes as food ingredients due to their high availability, biodegradability, renewable characters and functional properties such as biocompatibility; good amphiphilic properties; water solubility; and foaming, emulsifying, gelling and film-forming abilities (Quintero, Rojas, & Ciro, 2018). Among vegetable proteins commonly studied and widely used, we find soy (Salze, McLean, Battle, Schwarz, & Craig, 2010; Giri & Mangaraj, 2014), canola (Tan, Wang, & Moraru, 2014), pea (Fredrikson, Biot, Alminger, Carlsson, & Sandberg, 2001; Boye et al., 2010) and some pseudocereal proteins such as amaranth proteins (Aceituno-Medina, Mendoza, Lagaron, & López-Rubio, 2013). To serve as a food ingredient in dietary supplements, these macromolecules must be obtained in the form of highly purified fractions (biofunctional ingredients) with high commercial value.

Quinoa (*Chenopodium quinoa* Willd) is a South American dicotyledonous plant that is considered as pseudocereals since it is a broadleaf plant that has been used like the cereals. Quinoa seeds are recommended as an alternative high-quality protein resource because of their high protein content (12–23%) (Abugoch et al., 2009). There are two main globular storage proteins: 2S-type albumins (Alb) and 11S-type globulins, which are also known as chenopodins (Brinegar & Goundan, 1993; Brinegar, Bethel, & Nwokocha, 1996; Abugoch et al., 2009). The amino acid composition of this protein shows that it is high in cysteine, arginine, and histidine, which is why quinoa has a high nutritional value, although it has only recently been used as a novel functional food.

Quinoa protein isolates (QPI) can be traditionally prepared by extraction of the defatted flour with an alkaline solution (pH of 8 to 11) followed by acid precipitation (Elsohaimy, Refaay, & Zaytoun, 2015; Avila Ruiz, Arts, Minor, & Schutyser, 2016). Some authors have combined the effect of NaCl concentrations (0.0–1.0 M in 50 mM Tris-HC1, pH 8.0) and pH extract acidification (3.0–6.0) to increase the efficiency of chenopodin extraction (Brinegar & Goundan, 1993; Elsohaimy et al., 2015), since globulins are soluble proteins in saline solutions (Osborne, 1924). Other factors to consider in the extraction process optimisation are temperature, operation time, solid/solution ratio and stirring.

Traditional methods of producing protein concentrates, such as isoelectric precipitation, reduce oligosaccharides to negligible level but may contain large amounts of phytic acid (Ali, Ippersiel, Lamarche, & Mondor, 2010; Mondor, Ali, Ippersiel, & Lamarche, 2010) and insoluble

* Corresponding authors.
E-mail addresses: migdiarazo@ug.uchile.cl (M. Arazo), labugoch@uchile.cl (L. Abugoch), ctapia@uchile.cl (C. Tapia).

https://doi.org/10.1016/j.foodchem.2019.126154
Received 1 July 2019; Received in revised form 23 December 2019; Accepted 31 December 2019
Available online 07 January 2020
0308-8146/ © 2020 Elsevier Ltd. All rights reserved.

Nomenclature

UF	Ultrafiltration
UF_c	Centrifugal ultrafiltration
DV	Diavolume
DDF/UF	Discontinuous diafiltration/ultrafiltration
DF	Diafiltration
DF/UF	Diafiltration/ultrafiltration
MWCO	Molecular weight cutoff
ET	Quinoa total extract
UF_c-R_{30}	Centrifugal retentate for 30 kDa
UF_c-R_{100}	Centrifugal retentate for 100 kDa
UF_c-P_{30}	Centrifugal permeate for 30 kDa
UF_c-P_{100}	Centrifugal permeate for 100 kDa
DF_{30}	Diafiltrate for 30 kDa
DF_{100}	Diafiltrate for 100 kDa
C_{100}	Concentrate for 100 kDa
QPI	Quinoa protein isolate
2-ME	β-mercaptoethanol
VCF	Volumetric concentration factor
FF	Crossflow rate, mL/min
SDS-PAGE	Sodium dodecyl sulphate-polyacrylamide gel electrophoresis
TMP	Transmembrane pressure, kPa
Rt	Total resistance, m^{-1}
Rm	Clean membrane resistance, m^{-1}
Ri	Irreversible resistance, m^{-1}
Rr	Reversible resistance, m^{-1}
J_0	Initial flux, $L/h.m^2$
J	Permeate flux, $L/h.m^2$
J_0 exp	Experimental initial flux, $L/h.m^2$
Km	Cake filtration model constant, $s.m^{-2}$
Kp	Pore constriction model constant, m^{-1}
Ki	Intermediate blocking model constant, $s^{-0.5}m^{-0.5}$
Kc	Complete blocking model constant, s^{-1}

carbohydrates. In conventional methods, proteins are exposed to harsh conditions, which alter their functional properties. More recent findings have shown that membrane separation techniques, such as ultrafiltration (UF), can be used as an alternative to isoelectric precipitation to yield protein isolates with improved functionality. These membrane separation techniques can also be effectively used to remove some antinutritional components (Boye et al., 2010).

The major advantages of ultrafiltration are the high throughput of the product, relative ease of scale-up, and cleaning and sanitisation. One of the most widely used forms for protein separation by UF is crossflow filtration since large volumes of solution can be processed (Rosenberg, Hepbildikler, Kuhne, & Winter, 2009). However, these comparatively large sample volumes are usually not available during the early phases of development. Therefore, small scale techniques such as ultrafiltration that employ centrifugal filters can be used as alternatives in preformulation development (Shire, Shahrokh, & Liu, 2004). However, these batch processes are too difficult to scale up.

The major problem in UF applications is the limitation of the permeate flux to far below the pure solvent flux under the same pressure difference (Aimar, Howell, Clifton, & Sanchez, 1991). This limitation is a consequence of the accumulation of retained solutes at the surface of the membrane. During the ultrafiltration of macromolecular solutions, the increased solute concentration causes a rise in the osmotic pressure, which partially cancels the applied pressure difference. The basic working equation for the UF process is Darcy's law (Eq. (1)):

$$Jp = \frac{TMP}{\mu Rm} \quad (1)$$

where TMP is the transmembrane pressure, μ is the permeate viscosity and Rm is the resistance offered by the membrane.

Protein fractionation using ultrafiltration is still a challenge, and sometimes, it is not possible to remove all of a component from a feed using simple ultrafiltration. In this situation, diafiltration (DF) may be very useful. Extensive diafiltration should eventually reduce the concentration of low molecular weight compounds to very low levels (Grandison & Lewis, 1996). Diafiltration can be performed in combination with ultrafiltration to enhance either product yield or purity. DF is the fractionation process that washes smaller molecules through a membrane and leaves larger molecules in the retentate without ultimately changing concentration. There are two ways to perform diafiltration: continuous diafiltration, in which the diafiltration solution (water or buffer) is added to the sample feed reservoir at the same rate as permeate is generated, and discontinuous diafiltration, in which the solution is first diluted and then concentrated back to the starting volume (Grandison & Lewis, 1996).

Numerous studies report the separation of vegetal proteins by UF/DF techniques (Boye et al., 2010; Mondor et al., 2010). Navarro-Lisboa et al. (2017) evaluated the effect of the ultrafiltration process using ceramic membranes on physicochemical and conformational characteristics of quinoa protein fractions at two pH values above the isoelectric point of quinoa protein extracts. In such a study, various protein bands (17–95 kDa) were obtained in the concentrated sample, and the authors suggested a strategy to wash the concentrate stream using DF.

The objective of this work was to develop a scalable procedure using discontinuous DF/UF crossflow that allows us to obtain a purified fraction of chenopodin (55–57 kDa) with the same characteristics as that obtained by Ultra15 centrifugal filter devices at the bench scale since this batch process is difficult to scale up. The goal is to increase the protein yield for production volumes of the concentrate, shorten the processing time and develop a procedure using industrial equipment that allows for the production of high volumes of protein concentrate for their later use as food ingredients. Considering the native hexameric form of chenopodin (~320 kDa), the separation was achieved using a 30 kDa membrane followed by a 100 kDa membrane.

2. Material and methods

2.1. Materials

The seed flour of dehulled quinoa (*Chenopodium quinoa* Willd, from VI Region, Chile) used in this work was supplied by Promauka. The flour was stored at 4 °C until use. The following is the approximate composition of quinoa flour expressed per 100 g: the moisture was 11.3 g, protein 11.2 g, fat 4.9 g, ash 55.5 mg and carbohydrates 72.6 g (AOAC, 1995).

2.2. Preparation of quinoa protein extract

The protein extract was prepared according to Brinegar and Goundan (1993) by suspending the defatted flour in a buffer of 0.5 M NaCl/50 mM Tris-HCl pH 8.0 at a ratio of 1:10. The mixture is stirred for 1 h, and the suspension was centrifuged (HERMLE Z-323 Germany) and prefiltrated with a PVDF membrane of 0.45 μm (Durapore HVLP04700).

2.3. Isolation of 11S globulin by Ultra15 centrifugal filter devices (UF_c)

The 11S globulin fraction (56 kDa) –chenopodin– was obtained by UF_c, using Amicon Ultra15 tubes (Millipore, Cork, Ireland) with 30 and 100 kDa molecular weight cut-offs (MWCO) according to the procedure

described in Fig. 1. The membrane material was Ultracel® low binding regenerated cellulose. The sample in retentate was collected and stored at 4 °C for further analysis.

Quinoa protein fractions were labelled as ET (quinoa protein extract), UF_c-R_{30}, UF_c-R_{100}, UF_c-P_{100}, and UF_c-P_{30} according to the membrane cutoffs (30 or 100 kDa) and the R or P fraction (retentate or permeate). Samples were collected and stored at 4 °C for the analysis of the soluble protein content using the Bradford method and SDS-PAGE.

2.4. Crossflow equipment

A crossflow system (SARTOFLOW® Slice 200 Benchtop Crossflow System) was used with 30 and 100 kDa weight cut-off membranes (Sartocon® Slice 200 Hydrosart® Cassettes made of stabilized cellulose-based membrane). Data were collected using Win Wedge PC interface Software (TAL Technologies, Inc.). The membranes and system were thoroughly flushed with deionised distilled water before use to remove any residual storage agents.

2.5. Crossflow ultrafiltration performance and resistance-in series model

UF experiments were carried out in concentration mode (in which the concentrate is recirculated to the feed tank) with distilled water and quinoa protein fractions. The system was operated at room temperature (20 °C), and the crossflow rate (FF) was set to 50 mL/min. The permeability tests through both membranes were performed by measuring the permeate flux in litres per hour per metre squared (L/hm^2) at different transmembrane pressures (TMP). The transmembrane pressure (TMP) was varied by adjusting at five different pressure values.

During ultrafiltration of a solution under constant pressure, the permeation flux can be calculated using Equation (1), and it followed the resistance-in-series model. The resistance model assumes that flux (J) is proportional to transmembrane pressure (P) and inversely proportional to permeate viscosity (μ) and the membrane hydraulic resistance (Cheryan, 1998). For quinoa protein extract, the total resistance in a membrane system is the sum of the membrane and the fouling resistances (Eq. (2)):

$$Rt = Rm + Rr + Ri \quad (2)$$

Rm is determined from the water flux through a clean membrane, and the other resistances can be determined from permeation flux versus pressure data. Total resistance (Rt) is the sum of the clean membrane resistance (Rm), irreversible resistance (Ri) and reversible resistance (Rr). Together, the irreversible and reversible resistances represent the total fouling of the membrane.

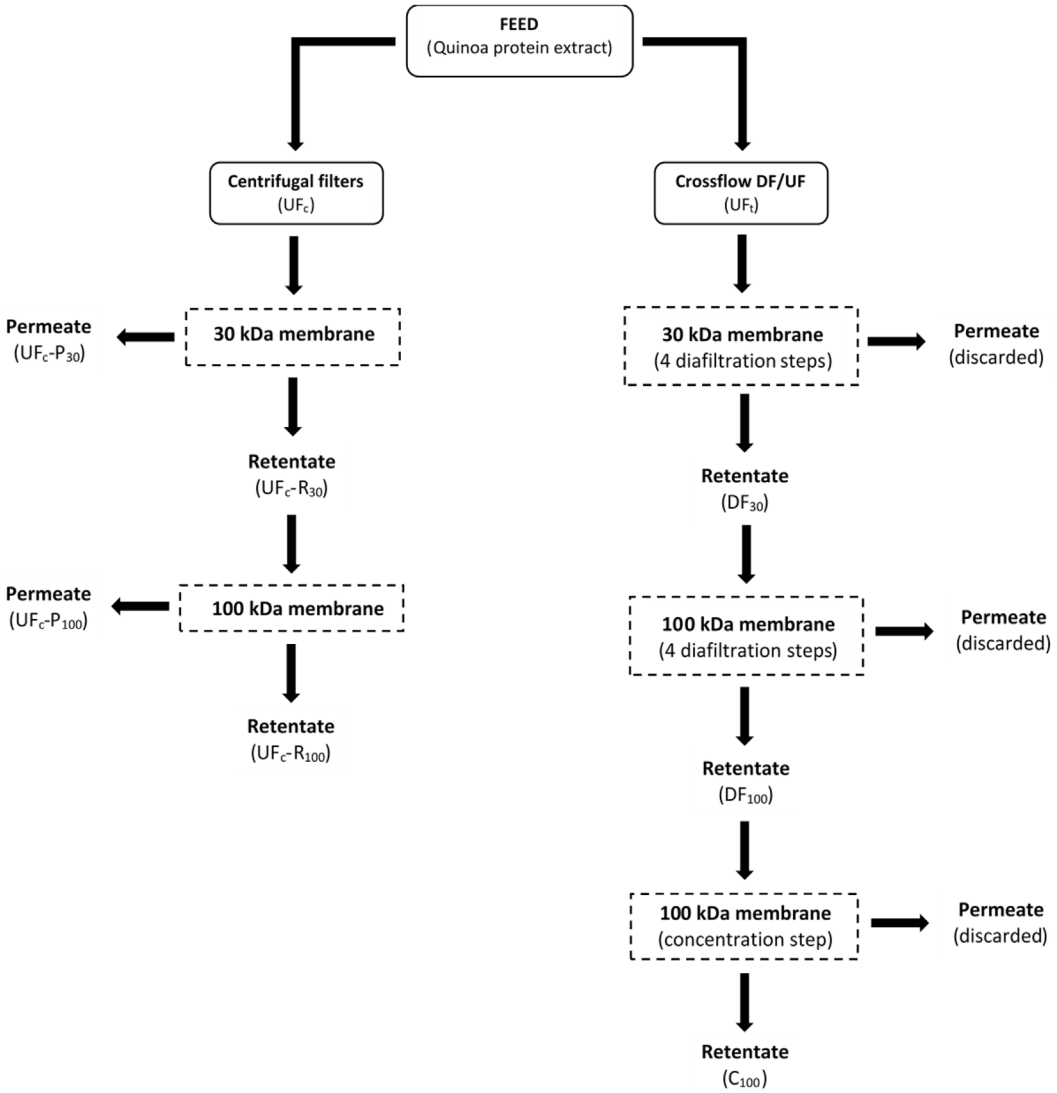

Fig. 1. General scheme for the processing and fractionation of quinoa protein by centrifugal filters (UFc) and crossflow UF (UFt) systems.

2.5.1. Diafiltration of the quinoa protein extract

Discontinuous diafiltration (DDF) experiments were run at a TMP of 10.34 kPa because this value was established in previous tests with quinoa protein extracts. Moreover, since the mechanism of fouling appears to be strongly dependent on the concentration polarization (Aimar et al., 1991), the samples were diluted in 4 diafiltration steps or diavolumes (4 DV). Diafiltration was initially performed with the 30 kDa membrane for which 200 mL of the extract was diluted with an equal volume of a buffer of 0.5 M NaCl/50 mM Tris-HCl, pH 8.0. Later, the diluted sample was concentrated back to its original volume by ultrafiltration, and this process was performed up to 4 DV. After this, the remaining retentate sample was processed for another four

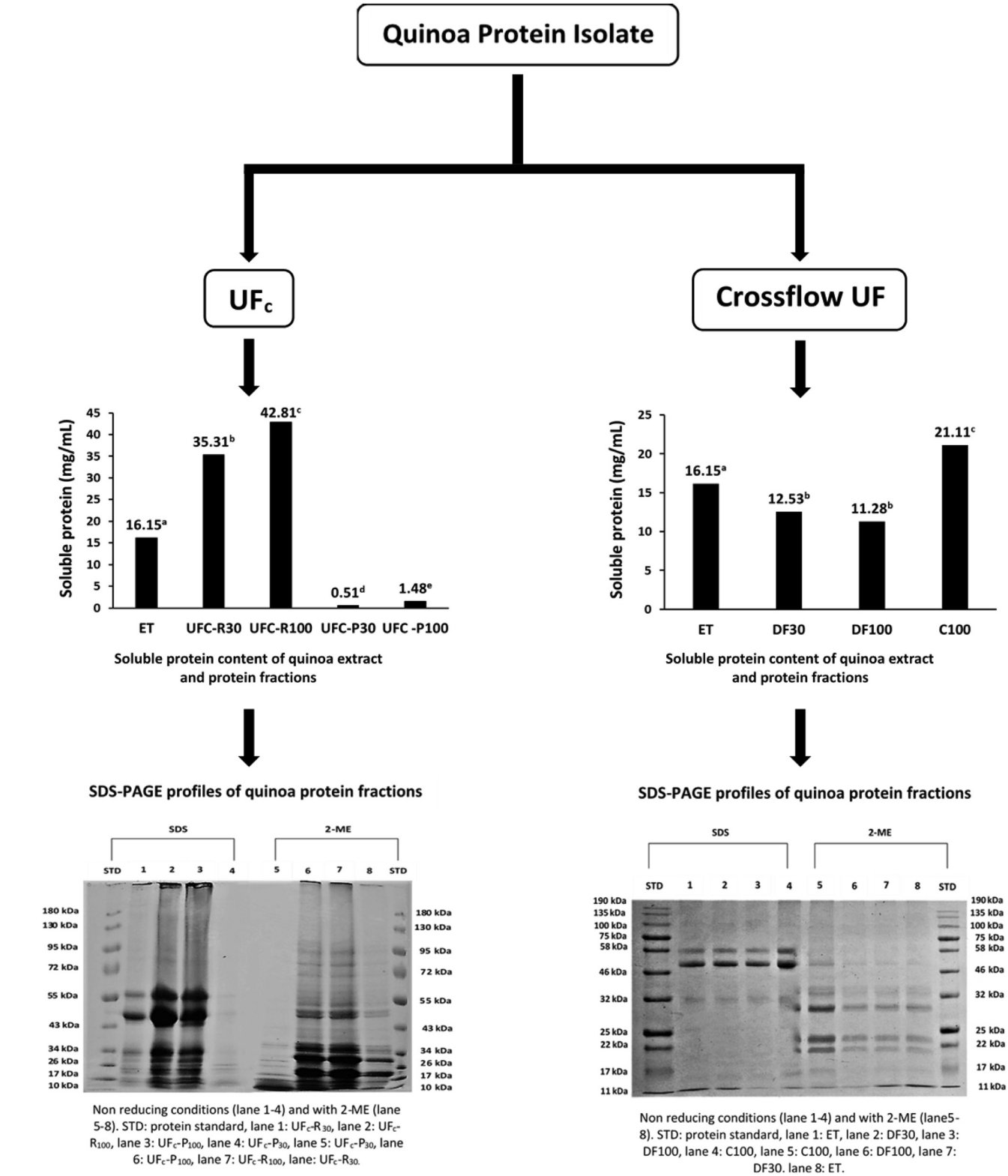

Fig. 2. Results of soluble protein and SDS-PAGE profiles of quinoa protein fractions obtained by centrifugal and crossflow UF systems. Different letters show significant differences ($p < 0.05$).

diafiltration steps with the 100 kDa membrane. Diafiltration samples were labelled as DF_{30} and DF_{100} according to the membrane cut-offs (30 or 100 kDa).

2.5.2. The concentration of the 11S globulin fraction

After the DDF steps with 30 and 100 kDa membranes, the diafiltrated sample (200 mL) was used as a feed solution in the final concentration using five different TMP values (as in the permeability tests) for selecting the critical TMP value. Concentration was performed with only the 100 kDa membrane, and the retentate was continuously recycled back to the feed tank until it reached 20% of the initial feed volume discarding the permeate. The final retentate sample was labelled as C_{100}.

All retentate samples in the crossflow DF/UF were collected as quinoa protein fractions and stored at 4 °C for subsequent analysis of the soluble protein concentrations and SDS-PAGE.

2.6. Modelling of fouling mechanisms during the concentration step using 100 kDa membrane

The contributions of the fouling mechanism or blocking pattern during the concentration process of the quinoa protein fraction were evaluated from the models developed by Hermia (1982). Hermia's models consider four main types of membrane fouling: complete blocking, intermediate blocking, standard blocking (pore constriction) and cake layer formation. The fit accuracy for each model was evaluated in terms of the regression coefficient (R^2_{adj}) and the standard deviation (SD).

2.7. SDS-PAGE analysis

Polyacrylamide gel electrophoresis (PAGE) was run on gel minislabs (Mini Protean III Model, Bio-Rad Laboratories, CA, USA) under nonreducing and reducing conditions. Sodium dodecyl sulfate (SDS)-PAGE were performed according to Laemmli (1970). SDS-PAGE gels contained 12% (w/v) acrylamide (5% acrylamide stacking gels). The molecular mass of the polypeptides was calculated using a molecular mass standard (blue prestained protein standard) from New England BioLabs with a broad range of 11–190 kDa (11, 17, 22, 25, 32, 46, 58, 75, 100, 135 and 190 kDa). The sample loading buffer contained 0.124 M Tris-HCl (pH 6.8), 15% (v/v) glycerol, and 2% (w/v) SDS. For reducing conditions, 5% (v/v) β-mercaptoethanol (2-ME) was added and the samples were heated (100 °C, 4 min). Protein bands were stained with Coomassie Brilliant Blue R.

2.8. Statistical analyses

All the results were expressed as the means with their corresponding standard deviation (SD) values. Data analysis was performed using Statgraphics Centurion XVI.II Statistical Software (Statistical Graphics Corp., Herdon, USA). Analysis of variance (ANOVA) tests were conducted by Fisher's least significant difference (LSD), and the differences were taken to be statistically significant when the p-value was < 0.05. All experiments and analytical measurements were conducted in triplicate.

3. Results and discussion

3.1. Soluble protein content and SDS profiles of the fractions obtained by ultrafiltration systems

The results presented in Fig. 2 show a significant increase ($p < 0.05$) in the protein concentration using the UF_c filters method for both membranes (30 and 100 kDa). Higher protein concentrations were detected in the retentates (35.31 and 48.81 mg/mL for UF_c-R_{30} and UF_c-R_{100}, respectively), whereas permeate samples showed lower protein contents (0.51 and 1.49 mg/mL for UF_c-P_{30} and UF_c-P_{100}, respectively). The initial protein content for the quinoa extract (ET) was 16.15 mg/mL, and thus, it was confirmed that UF is a suitable process to produce quinoa protein concentrates.

Centrifugal filters are commonly used in the fractionation and concentration procedure of monoclonal antibodies (Rosenberg et al., 2009; Eppler, Weigandt, Schulze, Hanefeld, & Bunjes, 2011) and other proteins of biological sources. There are just a few works that used UF in vegetable proteins (Balciunaite et al., 2015), and this is the first report that isolates quinoa protein using this technique to explore the possibilities of industrial scale-up.

In the crossflow system, the soluble protein content decreased after two diafiltration steps with the 30 and 100 kDa membranes (12.53 and 11.28 mg/mL for DF_{30} and DF_{100}, respectively). The first diafiltration step with the 30 kDa membrane removed, approximately 22.41% of proteins from the initial feed solution (16.15 mg/mL). Instead, the second diafiltration step removed only 9.98% of the proteins. This effect is probably due to the high retention of chenopodin hexamers. Throughout DDF, a buffer is continually introduced, and permeate removed from the system. Thus, the product (chenopodin) remains in the retentate, and low molecular weight components of extract go to into the permeate. Thereby exchanging buffers and reducing the concentration of albumin in the retentate. In the concentration step, the protein content of the C_{100} fraction increased significantly to a value of 21.11 mg/mL (Fig. 2), which represented 37.43% of the proteins in the diafiltrated feed.

SDS-PAGE analysis of UF_c protein fractions under nonreducing and reducing conditions showed a particularly high abundance of high molecular weight species (Fig. 2). The UF_c-R_{30}, UFC-R_{100} and UF_c-P_{100} samples showed identical electrophoresis patterns with different polypeptide groups with molecular weights between 14 and 63 kDa. The bands at 47 and 63 kDa were related to 11S globulin or chenopodin (Brinegar & Goundan, 1993; Abugoch et al., 2009). Under reducing conditions, most of these bands disappear resulting in other bands that correspond to the acid (31 kDa) and basic (25 kDa) subunits of the chenopodin. A globulin band has been found at approximately 55–57 kDa in quinoa protein isolates (Abugoch et al., 2009; Valenzuela, Abugoch, Tapia, & Gamboa, 2013) and in quinoa protein fractions obtained by ultrafiltration (Navarro-Lisboa et al., 2017). A soluble aggregate (an SDS nondissociable aggregate) was detected just above 180 kDa and in the wells (it was unable to enter the gel). Protein solutions whose concentrations are too high may precipitate out of solution and, once aggregated, will sit on the top of the running gel and not migrate. There are many situations in which the protein concentration or surface density becomes excessively high in the concentration processes, as well as in ultrafiltration, resulting in the aggregation and heterogeneity of protein solutions or inefficient processes. In particular, this can occur when using pressure-type or centrifugation-type devices. Loading proteins will be concentrated at the membrane surface leading to crowded conditions (Binabaji, Ma, Rao, & Zydney, 2016).

We mainly found bands of peptides of less than 34 kDa (30–34 kDa) in UF_c-R_{100} and UF_c-P_{100} fractions. Furthermore, all protein bands less than 20 kDa (14–18 kDa) corresponded to albumin components according to Brinegar et al. (1996), and in the UF_c-P_{30} fraction, this polypeptide band (14 kDa) increased the intensity under reducing conditions. This result is due to the extraction occurring at an alkaline pH in which the 11S globulin fractions might have been hydrolysed into fractions with lower molecular weights and associated through increased hydrophobic interactions and intermolecular disulfide bonds into aggregates (Valenzuela et al., 2013).

SDS profiles for crossflow UF fractions revealed the presence of the main bands at 57 and 50 kDa for the ET and the DF_{30}, DF_{100} and C_{100} fractions with high intensity in the concentrated sample (C_{100}). The classic acidic (31 kDa) and basic (21 and 23 kDa) subunits connected by disulfide bonds were disrupted in the presence of 2-ME. Under

nonreducing conditions, a protein band at 32 kDa was barely perceptible and corresponded to the acidic subunit of chenopodin. Alkali is known to cause disulfide bond cleavage, resulting in the dissociation of 11S globulin (Abugoch et al., 2009). The 11 kDa band (2S quinoa albumin) was barely visible in the DF_{100} and C_{100} samples but was highly prominent in ET and DF_{30} fractions. Thus, it was expected that proteins smaller than the membrane cut-off would pass through the permeate due to the selectivity of the membrane. Compared with the UF_c fractions, the strategy of washing the concentrate stream with several diafiltration steps improved the transmission of particles below the membrane cut-off. Hence, crossflow ultrafiltration allowed the isolation of quinoa 11S globulin having a molecular weight in the range of interest and the increase in their concentrations.

3.2. Diafiltration of the quinoa protein extract

In ultrafiltration, it is vital to maintain high permeate flux either in concentration or diafiltration. Nevertheless, this is a challenge straightforward to meet in diafiltration, since it requires us to diluted the feed. Thus, the protein concentration in the feed does not usually increase, and it maintains a relatively high permeate flux. In this case (Supplementary material: Fig. S1), diafiltration was carried out at constant pressure, and the permeate flux decreased with time due to membrane fouling. The permeate flux was reduced at the fourth stage of the diafiltration process for both MWCOs; however, it was sharply reduced for the 100 kDa membrane. This may be justified by the fact that, as time progresses, the concentration polarisation layer becomes thicker, which causes lower permeation as well as high resistance.

The 4 diafiltration steps lasted nearly 1 h for the 30 kDa membrane, while for the 100 kDa membrane, the duration was approximately 20 min. The permeate flux was lower with the decrease in MWCO because of the more compact nature of the membrane. As the MWCO of the membrane decreases, the smaller average pore size of the membrane resulted in higher membrane resistance and less permeability. Thus, the 30 kDa membrane has smaller pores than the 100 kDa membrane leading to a smaller flux and a longer diafiltration duration at a given pressure difference.

3.3. The concentration of the 11S globulin fraction

Fig. 3 shows the permeate flux and the concentration of protein versus TMP throughout the concentration stage. The relationships between permeate flux and TMP is close to linear until an approximate TMP value of 8.96 kPa is reached. Besides, at 12.41 kPa the flux decreased significantly, which suggests that the concentration polarisation/fouling is still negligible. In general, the permeate flux increases linearly with TMP up to some value of the TMP where a combination of the effects of concentration polarisation and fouling becomes significant (Bacchin et al., 2006). Due to the effect of concentration polarisation provoked a high osmotic pressure at the membrane surface. This osmotic pressure "subtracts" from the measured hydrostatic pressure difference across the membrane thereby reducing the solvent flux. Membrane fouling (i.e., membrane surface adsorption, membrane pore plugging, and gel layer formation on the membrane surface) could be explained through the formation of salt bridges between the membrane and quinoa proteins. Thus, fouling the membrane also reduces the flux (Ko & Pellegrino, 1992).

Moreover, when the applied TMP is under the required value (~8.96 kPa in this case) for the threshold flux of the membrane, the polarised layer on the membrane is dynamic and most rejected particles near the membrane surface are floating inducing an almost constant filtration resistance. Thus, the driving force will increase when the TMP rises. However, if the TMP exceeds the required value for the threshold flux, more retained particles may assemble leading to a more compacted fouling layer (Zhu et al., 2015).

The concentration of protein in the retentate (Fig. 3) increased with the increase in TMP (from 11.99 to 46.48 mg/mL). This effect may be explained due to the formation of a denser fouling layer at higher TMP. At higher TMP, more solute flows towards the membrane and the polarised layer acting as a secondary membrane promotes a higher rejection because of the higher compaction of the deposited solute layer (Sarkar, Ghosh, Dutta, Sen, & Bhattacharjee, 2009). Consequently, for the concentration of quinoa protein at 8.96 kPa (23.87 mg/mL) could be defined as a critical TMP above which data starts deviating from the linear regime and below which no membrane fouling occurs. However, considering that flux values at 8.96 and 10.34 kPa are not significantly different ($p < 0.05$), we decided to keep working at 10.34 kPa with higher protein content in the retentate (25.75 mg/mL).

The effects of time on permeate flux and volumetric concentration factor (VCF) at 10.34 kPa are shown in Fig. 4a. There was a gradual decrease in the initial permeate flux (0.55 L/h.m^2) with the time course when the VCF (the ratio between the feed volume and the volume of the retentate) increased because the concentration polarization and fouling phenomena reached a value of 0.38 L/h.m^2 (at the final time of 4 min). The VCF reached a maximum of 3.82 at approximately 20% of the initial 200 mL of the diafiltrated sample.

Permeate flux reduction is characteristic of the concentration mode tests as a consequence of the phenomena of concentration polarisation and/or membrane fouling, as explained before. Flux decline was attributed to the generated aggregates deposited on the membrane surface that caused pore clogging of the membrane resulting in less fluid being passed through the membrane (Grenier, Meireles, Aimar, & Carvin, 2008). According to several authors, the more concentrated the solution of protein the lower the permeate flux until a static condition is reached. Due to the higher osmotic pressure and the higher accumulation of solute molecules in the polarised layer, the flux thickness increases and, consequently, so does its resistance to permeation (Bacchin et al., 2006; Baldasso, Barros, & Tessaro, 2011).

Several types of fouling mechanisms could take place in a UF process. For this reason, it is necessary to obtain a model that predicts that permeate flux decline with time and determine the optimum operating conditions and, thus, minimise fouling in quinoa protein processing. Hermia's models and the resistance-in-series model were used to identify the most suitable fouling mechanism in the quinoa protein concentration process with the 100 kDa membrane.

3.3.1. Resistance-in-series model

The total resistance (Rt) of the 100 kDa membrane as a function of time for the concentration of quinoa protein fraction is shown in Supplementary material Fig. S2. The increase in Rt in the whole filtration process showed a linear performance because fouling occurs through a combination of different fouling mechanisms. This behaviour is in agreement with the results shown in Fig. 4a in which the declining permeate flux with time is one of the most critical limitations in filtration processes as feed components accumulate on the membrane

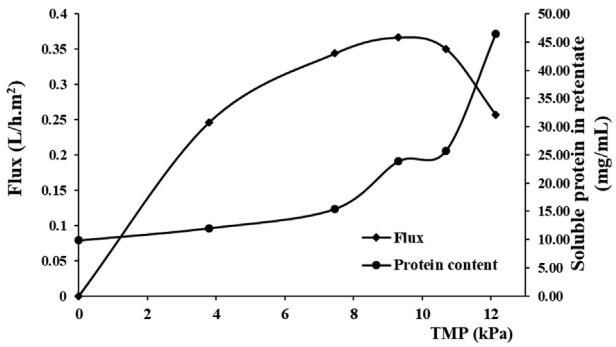

Fig. 3. Flux and soluble protein variations versus transmembrane pressure during concentration of the diafiltrated quinoa protein ($T_{average}$ = 20 °C; FF = 50 mL/min; 100 kDa membrane).

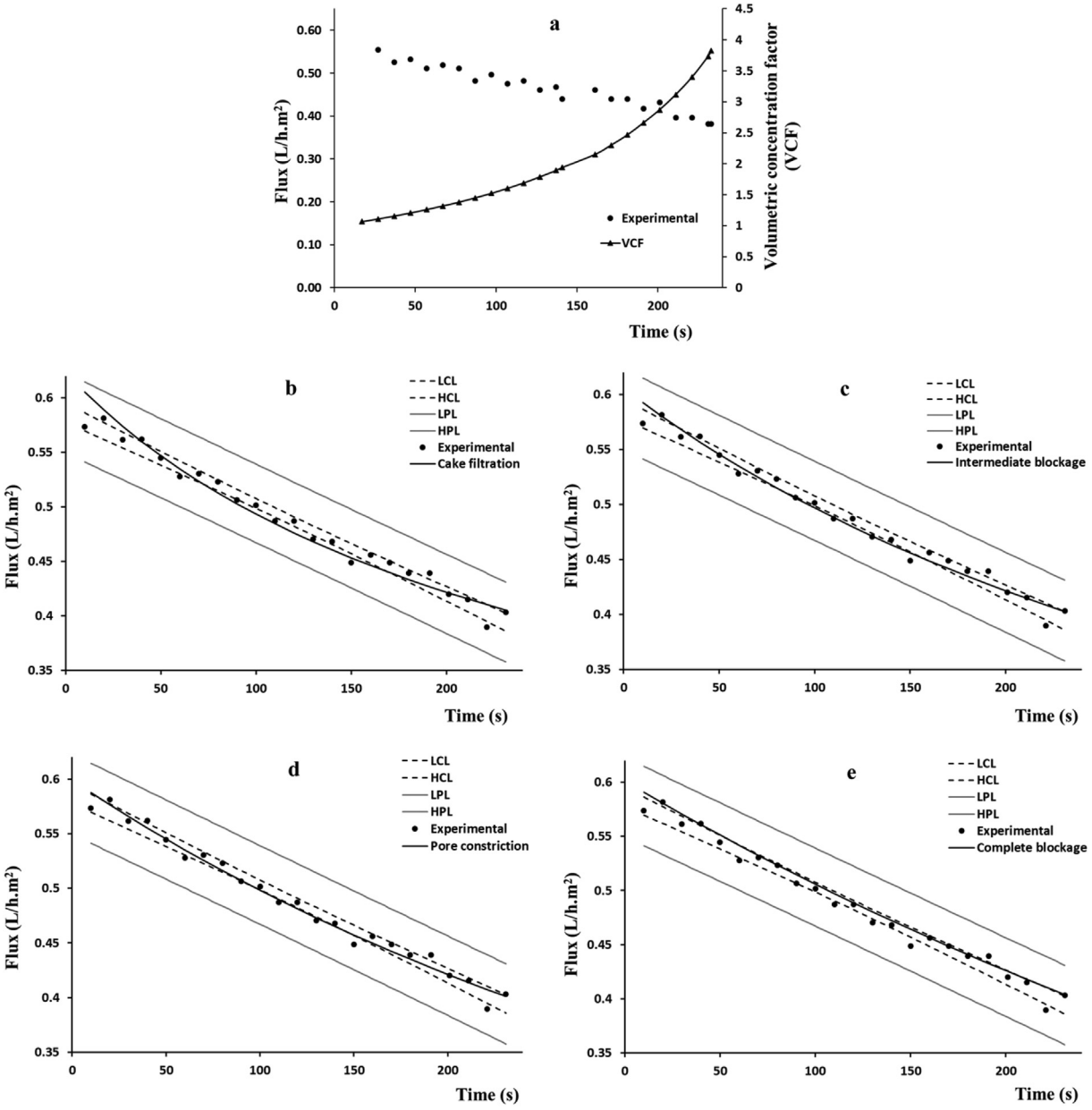

Fig. 4. Flux decline during concentration of the diafiltrated quinoa protein ($T_{average}$ = 20 °C; TMP = 10.34 kPa, FF = 50 mL/min; 100 kDa membrane). Variation in flux and VCF versus time (a), experimental flux and predicted flux by the cake filtration (b), intermediate blockage (c), pore constriction (d), and complete blockage (e) models. LCL: low confidence level, HCL: high confidence level, LPL: low predicted level, HPL: high predicted level.

surface resulting in a polarisation layer and possibly cake formation and pore plugging. However, the behaviour of the total resistance versus time curves alone does not provide clear information about the main fouling mechanism. Thus, the different fouling mechanisms can be distinguished using the resistance in the series model.

The fouling resistance contains the reversible fouling resistance (Rr) and the irreversible fouling resistance (Ri) (see Eq. (2)). The reversible fouling, including the concentration polarisation and part of the loosely attached deposit, was removed by rinsing the membrane with water. The remaining part of the deposit was considered as the irreversible fouling (due to adsorption and strongly attached foulants). At the end of the concentration process, the reversible resistance was the main resistance for the 100 kDa membrane (data not shown). The Rm and Ri showed values of 3.55×10^{9} and 4.11×10^{8} m^{-1}, respectively, while the Rr value was 9.67×10^{16} m^{-1}, which represented approximately 99.99% of the total resistance (1.00×10^{17} m^{-1}). These results demonstrated that the concentration polarisation and cake resistances are much more important for the total resistance than other effects. This is due to an increase in the concentration gradient of the protein in the bulk flow on the membrane surface with time, and this concentration increase created a gel layer that led to a greater aggregation phenomenon for proteins and consequently higher formation of a cake layer (Li, Zhao, Zhou, Xing, & Wong, 2007).

These results suggest that most of the loosely bound fouling part surface layer can be removed by physical means, such as relaxation and back-washing. Similar results were obtained by Mondor, Ippersiel, Lamarche, and Boye (2004) in the ultrafiltration performance of three soy protein extracts processed at different pH values. In this study, the resistance of both the concentrated layer and cake layer together was the primary resistance to the liquid permeation.

3.3.2. Modelling of fouling mechanisms during the concentration step using 100 kDa membrane

The fouling mechanism for the 100 kDa membrane at the TMP of 10.34 kPa was estimated by Hermia's model (Table 1), and the fit of the four models was evaluated in the light of the linear regression coefficient adjusted (R^2_{adj}). The values of the experimentally measured initial permeate flux (J_0 exp) and the initial permeate flux predicted by Hermia's models (J_0) are presented in Table 1.

Predicted values were more than the measured values, and the complete blockage and pore constriction models provided the best predictions for this parameter. However, the differences between measured and fitted values were lower than the experimental error of measurements. It can be observed that the predicted models (cake filtration, intermediate blocking, pore constriction and complete blocking) had similar coefficients, which seems to indicate that membrane fouling was caused by the simultaneous occurrence of multiple blocking mechanisms and concentration polarisation phenomena. Concentration polarisation is a boundary layer phenomenon established during operation of all pressure-driven membrane processes and is not taken into account in Hermia's model (Cassini, Tessaro, & Marczak, 2011). In general, all experimental data of permeate flux fit well in Hermia's models with all the R^2_{adj} values above 0.95. However, the best-fitting model for the experimental data was the complete blocking model (0.9973) followed by pore constriction and the intermediate blockage models.

For a better interpretation of the fouling phenomenon in the experimental tests with the concentration of quinoa protein isolate, the experimental data were fit to these models (Fig. 4b–e). It may be observed that the complete blockage mechanism matched almost all the experimental data quite satisfactorily during the whole process (Fig. 4e) followed by the pore constriction model (Fig. 4d), which also gave a close prediction with a value of 0.9938 for R^2_{adj} (Table 1). In this way, it was demonstrated that some blocking mechanism was governing the process. Fig. 4c shows the trend of the intermediate blockage model where it started to follow the experimental data approximately 20 s after the concentration process began. For the cake filtration model, the prediction of flux decline was close to the experimental data between 40 and 211 s (Fig. 4b). However, the initial flux decline data was overpredicted below 40 s.

Flux decline can be controlled by cake layer formation or pore blocking. When pore-blocking occurs, it can take place inside the pores (pore constriction) or outside of them (intermediate and complete blocking). In pore constriction, solute molecules (proteins) go entirely inside the membrane pores. If pore-blocking occurs outside the membrane pores, the molecules causing pore-blocking may have a similar size to the membrane pores and can be partially introduced into the membrane pores (intermediate blocking) or may be larger than the membrane pores (complete blocking) (Hermia, 1982). The complete blocking model considers that this type of fouling occurs when the size of the solute molecules in the feed solution is larger than the membrane pores. Therefore, solute molecules do not enter the membrane pores and do not arrive at the permeate side. In this study, the chenopodin molecule is a monomer with a molecular weight of 55–57 kDa. However, its native form is hexameric (~320 kDa) and thus it has a molecular size larger than the membrane pore size (100 kDa).

Numerous researchers have demonstrated the prevalence of a blocking mechanism when the pore sizes are relatively large. Rai, Majumdar, Sharma, Das Gupta, and De (2006) demonstrated that the flux decline in a 100 kDa membrane is the sharpest for the complete pore-blocking model among all the used UF membranes (including the 30 kDa membrane). Similar findings were obtained by Giri and Mangaraj (2014) during the evaluation of the effects of membrane pore size and pressure on soymilk ultrafiltration. Moreover, in the study by Corbatón-Báguena, Álvarez-Blanco, and Vincent-Vela (2015) complete blocking and cake formation were the predominant mechanisms for all the membranes and BSA feed solutions tested.

The values of fouling constants, or Hermia's model parameters (Km, Ki, Kp and Kc), for the fitted fouling mechanisms were applied in this work and are shown in Table 1. The high value of the cake formation parameter (2.21×10^{11} s.m^{-2}) could indicate that the extent of fouling contributed by the cake layer effect is significant, and this confirms that membrane fouling is a dynamic process with two distinctive stages: pore blockage that dominates at early filtration times followed by a cake layer mechanism that dominates at longer filtration times. In this way, it could be proposed that the flux starts to decline due to the deposit of native hexameric chenopodin on the membrane surface, which blocks the entrance of some pores completely. Simultaneously, some particles (low molecular species such as globulin dissociated monomers and dimers) with similar diameters to the membrane pores could deposit partially or entirely inside causing a progressive blocking of some pores during filtration. Finally, at approximately 40 s after the process starts, the particles continue depositing onto the membrane surface and form a cake.

The present findings seem to be consistent with the resistance-in-series model. When the concentration process is longer than approximately 40 s, external or reversible fouling mechanisms becomes important (complete blockage and cake filtration) avoiding a severe internal clogging.

In this study, the flux behaviour of a crossflow system was interpreted based on Hermia's models developed for dead-end filtration. It is important to consider the differences between crossflow and dead-end filtration. In crossflow filtration, the feed solution flows parallel to the membrane surface, and, in dead-end filtration, the feed solution flows perpendicular to the membrane surface. Nevertheless, in both flow configurations (dead-end and crossflow) the driving force is perpendicular to the membrane surface. Thus, it is possible to consider that the type of fouling included in Hermia's models for dead-end filtration may also occur in crossflow filtration (Cassini et al., 2011). Besides, permeate flux in crossflow filtration is nearly constant and decreases very slowly until a permeate flux of zero is obtained for very long time scales. This can explain the fact that, in crossflow filtration, the steady-state condition does not take place in a rigorous way but a quasi-steady-state condition occurs in actual applications. Hermia's models have been used for experimental data obtained through crossflow UF because

Table 1
Hermia's model parameters and R^2_{adj} values from the experimental data in quinoa protein fraction concentration using the 100 kDa membrane.

Fouling mechanisms	Linear equation	J_0 (L/hm^2)	K-value*	R^2_{adj}	J_0 exp (L/h.m^2)
Cake filtration model (n = 0)	$\frac{1}{J2} = \frac{1}{J02} + Km * t$	0.64 ± 0.01	2.21 ± 0.06	0.9729	0.57 ± 0.02
Intermediate blockage (n = 1)	$\frac{1}{J} = \frac{1}{J0} + Ki * t$	0.61 ± 0.00	14450.91 ± 221.56	0.9888	
Pore constriction (n = 1.5)	$\frac{1}{J0.5} = \frac{1}{J00.5} + Kp * t$	0.60 ± 0.02	2.62 ± 0.03	0.9938	
Complete blockage (n = 2)	$LnJ = LnJ0 + Kc * t$	0.60 ± 0.00	1.91 ± 0.03	0.9973	

The values were represented as the mean ± standard deviation (n = 3).

* Resistance coefficient filtration models: Cake filtration, Km ($\times 10^{11}$ s m^{-2}); Intermediate blockage, Ki (m^{-1}); Pore constriction, Kp (s$^{-0.5}$m$^{-0.5}$); Complete blockage, Kc ($\times 10^{-3}$ s^{-1}).

these models can predict the membrane fouling at different experimental conditions with precision.

3.4. Comparison between centrifugal and crossflow UF processes for the isolation of quinoa protein

In this study, the centrifugal filtration could achieve the highest concentration (42.81 mg/mL), although the most rapid concentration was observed for crossflow filtration. It took a very long time to reach high protein concentrations by using Ultra15 centrifugal filter devices, and the handling was more difficult (Table 2). To obtain approximately 844.40 mg of protein per 40 mL of a final concentrate of chenopodin through crossflow ultrafiltration, only 1.5 h was required, while Ultra15 centrifugal filter devices technique produced 17.12 mg in approximately 33.66 hrs. Also, is important to point out that, in centrifugal techniques, 100 steps of spin time with the 30 kDa membrane are necessary to reach the 15 mL needed for filtration with 100 kDa.

The UF_c technique only required 15 mL to achieve a higher concentration, which was a smaller amount of material than in crossflow filtration. This is because the Ultra15 centrifugal filter devices can be refilled with the concentrated protein solution, and the process can be repeated. The starting volume of the sample for crossflow UF was limited to only 200 mL since higher starting volumes limited the high concentration by the viscosity of the concentrated solution (Shire et al., 2004).

In terms of protein recovery, the crossflow UF appeared more effective than the centrifugal filters method by recovering 26.14% of the total protein solubilised by the alkaline buffer extraction of the quinoa flour. A high retention rate of protein was found in the concentration of the diafiltrated quinoa fraction with a value of 98.75% (data not shown). The protein quantity (844.4 mg) obtained through the crossflow DF/UF system represented 37.70% of the total protein, which is comparable with the results of Bringer, Bethel, & Nwokocha (1996) who found that chenopodin as one of the major storage protein fractions purified by gel filtration (37% of the total protein). The low protein yield value is due to the washing effect during the DF steps transmitting a significant proportion of molecules with a molecular weight lower than the membrane cut-off in the permeate such as the albumin (11–14 kDa) and another low molecular species. It is possible to recover more albumin in the permeate by increasing the diavolumes in diafiltration up to a certain point where the protein recovery will no longer be significant. Hence, this percentage of protein yield is a rate between the chenopodin fraction (mg) and the total protein content in the extract (feed). Nevertheless, it must be considered that the protein loss caused by its participation in membrane fouling and the foam formation during the concentration process.

The crossflow cassettes have a larger area than the Ultra15 centrifugal filter devices, and this is why the crossflow system can process higher volumes of feed per unit of area and time (7.25 L/h.m^2) than the centrifugal UF process (0.59 L/h.m^2). The Sartocon® Slice 200 filter cassettes are the same as larger Sartorius Stedim Biotech Sartocon® 0.1 m^2 or 0.7 m^2 production scale cassettes. Therefore, this result provides helpful information and predictable performance for linear upscaling, as well as future production requirements for chenopodin separation.

On the other hand, SDS PAGE analysis revealed some differences in the concentration techniques (Fig. 2), whereas the UF_c technique caused heterogeneity in the bands with the formation of soluble aggregates. A reason for this might be the dilution steps during diafiltration with both membranes. It is well known that DF is used for protein purification to eliminate problems associated with high concentrations in the retained product, generating high purification, while retaining a good performance process (Ebersold & Zydney, 2004). The crossflow reduces the sticking of protein to the membrane avoiding a “dead end” filtration situation. Consequently, it can avoid the blocking of the membrane and the formation of aggregates caused by the extremely high concentrations of protein that can build up in the gel and polarization boundary layer near the membrane (Rosenberg et al., 2009).

4. Conclusions

In summary, the best results concerning the highest achievable concentration and quality of the chenopodin were observed for the crossflow UF method. This technique was the most efficient and easy to handle, resulting in a shorter concentration time. These results are the first that show the isolation of 57 kDa quinoa fraction by using the crossflow system preceded with diafiltration steps. Although the use of Ultra15 centrifugal filter devices resulted in higher protein concentration, this method showed the formation of soluble aggregates.

Crossflow ultrafiltration is an attractive technique for quinoa protein processing, and the DF/UF technique is suggested for scaling-up for industrial purposes. Nevertheless, further work is required in this area. It is recommended that the application of a continuous UF with diafiltration steps after sample concentration is used because this way requires a lower volume of diafiltration buffer.

According to the resistance in the series model and the four membrane blocking models proposed by Hermia, the experimental data pointed to the concentration polarisation and cake filtration as the predominant fouling mechanisms. Hence, under similar conditions, this method can predict membrane flux in the scale-up crossflow ultrafiltration equipment for quinoa extract. A systematic membrane cleaning and pretreatment of the feed (quinoa protein extract) are crucial for controlling membrane fouling. Reducing membrane fouling is still an important research goal for achieving membrane processes that are more efficient and to obtain higher quality products.

The present study highlights the opportunities to produce 11S globulin from quinoa seed for use as a foods ingredient.

Table 2
Comparison of some technical parameters for the centrifugal and crossflow UF for quinoa protein isolation.

Parameters	UF_c		Crossflow UF	
			DDF	Concentración
	30 kDa	100 kDa	30 y 100 kDa	100 kDa
Feed volume (mL)	15	15	200	200
Operating time (h)	33.33	0.33	1.32	0.06
J (L/hm^2)	0.59		7.25	
Final concentrate volume (mL)	0.15	0.4	200	40
Soluble protein content in final concentrate (mg/mL)	42.81		21.11	
Milligrams of protein in final concentrate	17.12		844.40	
Protein yield (%)*	1.06		26.14	

* mg of protein in final concentrate /mg of protein in the feed (extract).

CRediT authorship contribution statement

Migdalia Arazo: Methodology, Investigation, Data curation, Writing - original draft, Visualization. **Nestor Jaque:** Formal analysis, Investigation, Software, Validation. **Nelson Caro:** Formal analysis, Validation. **Lilian Abugoch:** Methodology, Supervision, Writing - review & editing. **Cristian Tapia:** Conceptualization, Data curation, Supervision, Writing - review & editing.

Declaration of Competing Interest

The authors declare that they have no known competing financial interests or personal relationships that could have appeared to influence the work reported in this paper.

Acknowledgements

This work was supported by the Comisión Nacional de Investigación Científica y Tecnológica Grant numbers: CONICYT-PCHA/Doctorate National/2015-folio 21150356, Corporación de Fomento de la Producción Grant numbers: INNOVA CORFO 12IDL2-13621 Universidad de Chile Grant numbers: Project PEEI. 2nd version 2017.

Appendix A. Supplementary data

Supplementary data to this article can be found online at https://doi.org/10.1016/j.foodchem.2019.126154.

References

Abugoch, L., Castro, E., Tapia, C., Añón, M. C., Gajardo, P., & Villarroel, A. (2009). Stability of quinoa flour proteins (*Chenopodium quinoa* Willd.) during storage. *International Journal of Food Science and Technology, 44*(10), 2013–2020. https://doi.org/10.1111/j.1365-2621.2009.02023.x.

Aceituno-Medina, M., Mendoza, S., Lagaron, J. M., & López-Rubio, A. (2013). Development and characterization of food-grade electrospun fibers from amaranth protein and pullulan blends. *Food Research International, 54*(1), 667–674. https://doi.org/10.1016/j.foodres.2013.07.055.

Aimar, P., Howell, J. A., Clifton, M. J., & Sanchez, V. (1991). Concentration polarisation build-up in hollow fibers: A method of measurement and its modelling in ultrafiltration. *Journal of Membrane Science, 59*(1), 81–99. https://doi.org/10.1016/S0376-7388(00)81223-5.

Ali, F., Ippersiel, D., Lamarche, F., & Mondor, M. (2010). Characterization of low-phytate soy protein isolates produced by membrane technologies. *Innovative Food Science and Emerging Technologies, 11*(1), 162–168. https://doi.org/10.1016/j.ifset.2009.08.004.

AOAC 942.15. (1995). Official methods of analysis of AOAC international (16th ed; P. A. Cunniff & AOAC International, eds.). Gaithersburg, MD: Association of Official Analytical Chemists.

Avila Ruiz, G., Arts, A., Minor, M., & Schutyser, M. (2016). A hybrid dry and aqueous fractionation method to obtain protein-rich fractions from quinoa (*Chenopodium quinoa* Willd). *Food and Bioprocess Technology, 9*(9), 1502–1510. https://doi.org/10.1007/s11947-016-1731-0.

Bacchin, P., Aimar, P., Field, R., Bacchin, P., Aimar, P., & Critical, R. F. (2006). Critical and sustainable fluxes: Theory, experiments and applications To cite this version: HAL Id: Hal-00201119 review critical and sustainable fluxes: Theory, experiments and applications. *Journal of Membrane Science, 281*(1–2), 42–69. https://doi.org/10.1016/j.memsci.2006.04.014. <hal-00201119>.

Balciunaite, G., Juodsnukyte, J., Savickas, A., Ragazinskiene, O., Siatkute, L., Zvirblyte, G., ... Savickiene, N. (2015). Fractionation and evaluation of proteins in roots of *Echinacea purpurea* (L.) Moench. *Acta Pharmaceutica, 65*(4), 473–479. https://doi.org/10.1515/acph-2015-0036.

Baldasso, C., Barros, T. C., & Tessaro, I. C. (2011). Concentration and purification of whey proteins by ultrafiltration. *Desalination, 278*(1–3), 381–386. https://doi.org/10.1016/j.desal.2011.05.055.

Binabaji, E., Ma, J., Rao, S., & Zydney, A. L. (2016). Ultrafiltration of highly concentrated antibody solutions: Experiments and modeling for the effects of module and buffer conditions. *Biotechnology Progress, 32*(3), 692–701. https://doi.org/10.1002/btpr.2252.

Boye, J. I., Aksay, S., Roufik, S., Ribéreau, S., Mondor, M., Farnworth, E., & Rajamohamed, S. H. (2010). Comparison of the functional properties of pea, chickpea and lentil protein concentrates processed using ultrafiltration and isoelectric precipitation techniques. *Food Research International, 43*(2), 537–546. https://doi.org/10.1016/j.foodres.2009.07.021.

Brinegar, C., Bethel, S., & Nwokocha, L. (1996). High-cysteine 2s seed storage proteins from quinoa (*Chenopodium quinoa*). *Journal of Agricultural and Food Chemistry, 44*(7), 1621–1623. https://doi.org/10.1021/jf950830+.

Brinegar, C., & Goundan, S. (1993). Isolation and characterization of chenopodin, the 11S seed storage protein of quinoa (*Chenopodium quinoa*). *Journal of Agricultural and Food Chemistry, 41*(2), 182–185. https://doi.org/10.1021/jf00026a006.

Cassini, A. S., Tessaro, I. C., & Marczak, L. D. F. (2011). Ultrafiltration of wastewater from isolated soy protein production: Fouling tendencies and mechanisms. *Separation Science and Technology, 46*(7), 1077–1086. https://doi.org/10.1080/01496395.2010.551045.

Cheryan, M. (1998). Ultrafiltration and microfiltration handbook (2nd ed.). https://doi.org/10.1201/9781482278743.

Corbatón-Báguena, M. J., Álvarez-Blanco, S., & Vincent-Vela, M. C. (2015). Fouling mechanisms of ultrafiltration membranes fouled with whey model solutions. *Desalination, 360*, 87–96. https://doi.org/10.1016/j.desal.2015.01.019.

Ebersold, M. F., & Zydney, A. L. (2004). The effect of membrane properties on the separation of protein charge variants using ultrafiltration. *Journal of Membrane Science, 243*(1–2), 379–388. https://doi.org/10.1016/j.memsci.2004.06.043.

Elsohaimy, S. A., Refaay, T. M., & Zaytoun, M. A. M. (2015). Physicochemical and functional properties of quinoa protein isolate. *Annals of Agricultural Sciences, 60*(2), 297–305. https://doi.org/10.1016/j.aoas.2015.10.007.

Eppler, A., Weigandt, M., Schulze, S., Hanefeld, A., & Bunjes, H. (2011). Comparison of different protein concentration techniques within preformulation development. *International Journal of Pharmaceutics, 421*(1), 120–129. https://doi.org/10.1016/j.ijpharm.2011.09.028.

Fredrikson, M., Biot, P., Alminger, M. L., Carlsson, N. G., & Sandberg, A. S. (2001). Production process for high-quality pea-protein isolate with low content of oligosaccharides and phytate. *Journal of Agricultural and Food Chemistry, 49*(3), 1208–1212. https://doi.org/10.1021/jf000708x.

Giri, S. K., & Mangaraj, S. (2014). Soymilk concentration by ultrafiltration: Effects of pore size and transmembrane pressure on filtration performance. *International Journal of Food Science and Technology, 49*(3), 666–672. https://doi.org/10.1111/ijfs.12348.

Grandison, A. S., & Lewis, M. J. (1996). Separation processes in the food and biotechnology industries: Principles and applications. In A. S. Grandison, & M. J. Lewis (Eds.). *Carbohydrate polymers*(1st ed.). Woodhead Publishing Limited.

Grenier, A., Meireles, M., Aimar, P., & Carvin, P. (2008). Analysing flux decline in dead-end filtration. *Chemical Engineering Research and Design*.

Hermia, J. (1982). Constant pressure blocking filtration laws – Application to power-law non-Newtonian fluids. *Transactions Institute of Chemical Engineers, 60*(3), 183–187.

Ko, M. K., & Pellegrino, J. J. (1992). Determination of osmotic pressure and fouling resistance and their effects of performance of ultrafiltration membranes. *Journal of Membrane Science, 74*(1–2), 141–157. https://doi.org/10.1016/0376-7388(92)87079-D.

Laemmli, U. K. (1970). Cleavage of structural proteins during the assembly of the head of bacteriophage T4. *Nature, 228*(October 17th), 227–231.

Li, M., Zhao, Y., Zhou, S., Xing, W., & Wong, F. S. (2007). Resistance analysis for ceramic membrane microfiltration of raw soy sauce. *Journal of Membrane Science, 299*(1–2), 122–129. https://doi.org/10.1016/j.memsci.2007.04.033.

Mondor, M., Ali, F., Ippersiel, D., & Lamarche, F. (2010). Impact of ultrafiltration/diafiltration sequence on the production of soy protein isolate by membrane technologies. *Innovative Food Science and Emerging Technologies, 11*(3), 491–497. https://doi.org/10.1016/j.ifset.2010.02.002.

Mondor, M., Ippersiel, D., Lamarche, F., & Boye, J. I. (2004). Production of soy protein concentrates using a combination of electroacidification and ultrafiltration. *Journal of Agricultural and Food Chemistry, 52*(23), 6991–6996. https://doi.org/10.1021/jf0400922.

Navarro-Lisboa, R., Herrera, C., Zúñiga, R. N., Enrione, J., Guzmán, F., Matiacevich, S., & Astudillo-Castro, C. (2017). Quinoa proteins (*Chenopodium quinoa* Willd.) fractionated by ultrafiltration using ceramic membranes: The role of pH on physicochemical and conformational properties. *Food and Bioproducts Processing, 102*, 20–30. https://doi.org/10.1016/j.fbp.2016.11.005.

Osborne, T. B. (1924). The Vegetable Proteins. In Science (Vol. 32). https://doi.org/10.1126/science.32.821.409.

Quintero, J., Rojas, J., & Ciro, G. (2018). Vegetable proteins as potential encapsulation agents: A review. Retrieved from *Foodresearch, 2*(3), 208–220. http://www.myfoodresearch.com/uploads/8/4/8/5/84855864/_1_fr-2017-261_quintero_2.pdf.

Rai, P., Majumdar, G. C., Sharma, G., Das Gupta, S., & De, S. (2006). Effect of various cutoff membranes on permeate flux and quality during filtration of mosambi (*Citrus Sinensis* (L.) Osbeck) juice. *Food and Bioproducts Processing, 84*(3), 213–219. https://doi.org/10.1205/fbp.05181.

Rosenberg, E., Hepbildikler, S., Kuhne, W., & Winter, G. (2009). Ultrafiltration concentration of monoclonal antibody solutions: Development of an optimized method minimizing aggregation. *Journal of Membrane Science, 342*(1–2), 50–59. https://doi.org/10.1016/j.memsci.2009.06.028.

Salze, G., McLean, E., Battle, P. R., Schwarz, M. H., & Craig, S. R. (2010). Use of soy protein concentrate and novel ingredients in the total elimination of fish meal and fish oil in diets for juvenile cobia, *Rachycentron canadum*. *Aquaculture, 298*(3–4), 294–299. https://doi.org/10.1016/j.aquaculture.2009.11.003.

Sarkar, P., Ghosh, S., Dutta, S., Sen, D., & Bhattacharjee, C. (2009). Effect of different operating parameters on the recovery of proteins from casein whey using a rotating disc membrane ultrafiltration cell. *Desalination, 249*(1), 5–11. https://doi.org/10.1016/j.desal.2009.06.007.

Shire, S. J., Shahrokh, Z., & Liu, J. U. N. (2004). Challenges in the development of high protein concentration formulations. *Journal of Pharmaceutical Sciences, 93*(6), 1390–1402.

Tan, T. J., Wang, D., & Moraru, C. I. (2014). A physicochemical investigation of membrane fouling in cold microfiltration of skim milk. *Journal of Dairy Science, 97*(8), 4759–4771. https://doi.org/10.3168/jds.2014-7957.

Valenzuela, C., Abugoch, L., Tapia, C., & Gamboa, A. (2013). Effect of alkaline extraction on the structure of the protein of quinoa (*Chenopodium quinoa* Willd.) and its influence on film formation. *International Journal of Food Science and Technology, 48*(4), 843–849. https://doi.org/10.1111/ijfs.12035.

Zhu, Z., Liu, Y., Guan, Q., He, J., Liu, G., Li, S., ... Jaffrin, M. Y. (2015). Purification of purple sweet potato extract by dead-end filtration and investigation of membrane fouling mechanism. *Food and Bioprocess Technology, 8*(8), 1680–1689. https://doi.org/10.1007/s11947-015-1532-x.